The Aesthetic Surgery Education and Research Foundation

Breast Surgery

Histologic, Molecular, and Clinical Evaluation of Explanted Breast Prostheses, Capsules, and Acellular Dermal Matrices for Bacteria

Aesthetic Surgery Journal
2015, Vol 35(6) 653–668

DOI: 10.1093/asj/sjv017
www.aestheticsurgeryjournal.com
OXFORD UNIVERSITY PRESS

Louis Poppler, MD; Justin Cohen, MD, MS; Utku Can Dolen, MD; Andrew E. Schriefer, BA; Marissa M. Tenenbaum, MD; Corey Deeken, PhD; Richard A. Chole, MD, PhD; and Terence M. Myckatyn, MD, FRCSC, FACS

Abstract

Background: Subclinical infections, manifest as biofilms, are considered an important cause of capsular contracture. Acellular dermal matrices (ADMs) are frequently used in revision surgery to prevent recurrent capsular contractures.

Objective: We sought to identify an association between capsular contracture and biofilm formation on breast prostheses, capsules, and ADMs in a tissue expander/implant (TE/I) exchange clinical paradigm.

Methods: Biopsies of the prosthesis, capsule, and ADM from patients ($N = 26$) undergoing TE/I exchange for permanent breast implant were evaluated for subclinical infection. Capsular contracture was quantified with Baker Grade and intramammary pressure. Biofilm formation was evaluated with specialized cultures, rtPCR, bacterial taxonomy, live:dead staining, and scanning electron microscopy (SEM). Collagen distribution, capsular histology, and ADM remodeling were quantified following fluorescent and light microscopy.

Results: Prosthetic devices were implanted from 91 to 1115 days. Intramammary pressure increased with Baker Grade. Of 26 patients evaluated, one patient had a positive culture and one patient demonstrated convincing evidence of biofilm morphology on SEM. Following PCR amplification 5 samples randomly selected for 16S rRNA gene sequencing demonstrated an abundance of suborder Micrococcineae, consistent with contamination.

Conclusions: Our data suggest that bacterial biofilms likely contribute to a proportion, but not all diagnosed capsular contractures. Biofilm formation does not appear to differ significantly between ADMs or capsules. While capsular contracture remains an incompletely understood but common problem in breast implant surgery, advances in imaging, diagnostic, and molecular techniques can now provide more sophisticated insights into the pathophysiology of capsular contracture.

Level of Evidence: 4

Accepted for publication January 27, 2015.

Drs Poppler and Dr Cohen are Residents, Dr Dolen is a Breast Fellow, Dr Tenenbaum is Residency Program Director and Assistant Professor, and Dr Myckatyn is Breast Fellowship Director and Associate Professor, Division of Plastic and Reconstructive Surgery, Washington University School of Medicine, Saint Louis, MO. Mr. Schriefer is a Physicist, Genome Technology Access Center, Department of Genetics, Washington University School of Medicine, Saint Louis, MO.
Dr Deeken is Director of Biomedical Engineering and Biomaterials Laboratory, Department of Surgery, Section of Minimally Invasive Surgery, Washington University School of Medicine, Saint Louis, MO. and Dr Chole is Lindburg Professor and Chairman, Department of Otolaryngology, and Director of the Biofilm Core Facility, Washington University School of Medicine, Saint Louis, MO.

Corresponding Author:
Dr Terence M. Myckatyn, Washington University School of Medicine, 1040 N. Mason, Suite 124, Saint Louis, MO 63141, USA.
E-mail: myckatyn@wudosis.wustl.edu

Capsular contracture (CC) is the most common cause of implant failure in cosmetic and reconstructive breast surgery.[1] Proposed mechanisms for CC continue to evolve, usually implicating an upstream inflammatory event leading to abnormal downstream collagen or myofibroblast deposition.[2-10] While several CC studies investigated signaling pathways mediated by transforming growth factor-ß (TGF-ß),[3] tumor necrosis factor-stimulated gene-6 (TSG-6),[5] or leukotriene antagonist-mediated immunomodulation,[8,11,12] others focused on the impact of subclinical infection or biofilms.[13-21] An association between bacteria and CC is supported by studies implementing increasingly sophisticated culture techniques,[19] recently accompanied by electron and confocal microcopy, and molecular biology.[13,14,16,18] Techniques mitigating periprosthetic bacterial contamination that reduce the rate of CC support this association.[14,22,23]

Retrospective reviews and technique papers have suggested that acellular dermal matrices (ADMs) reduce CC in revision breast augmentation.[24-26] In primates, ADMs contain less smooth muscle actin compared to capsule, suggesting that ADMs may provide a barrier to the host inflammatory response.[27] In humans, ADMs are characterized by less granulation tissue, vascular proliferation, fibrosis, chronic inflammation, and fewer giant cells.[28] The primary purpose of this prospective cross-sectional study was to identify biofilms on the surface of textured tissue expanders (TEs), ADMs, and the submuscular capsule at the time of implant exchange during prosthetic breast reconstruction. We hypothesized that patients with Baker Grade III or greater CC would be more likely to have a biofilm present than patients with lower Baker Grades. The secondary purpose of this study was to describe the cellular populations and collagen type in patients with various levels of CC. We hypothesized that patients with CC will demonstrate an increased cellularity, and an altered ratio of type I to type III collagen in both capsular tissue and incorporated ADM.[2,29]

METHODS

Patient Selection

Of 147 women undergoing exchange of a TE for a breast implant (TE/I) with authors (TMM, MMT) at the Washington University School of Medicine from Jan 2013 to June 2014, 63 were randomly selected for participation.[30] Randomization was performed with software available online through www.randomizer.org[30] (Wesleyan University, Middletown, Connecticut, USA).

Twenty-six patients who received radiation, chemotherapy, endocrine therapy, or who had a previous flap or soft tissue envelope so thin that a biopsy would cause contour deformity, were excluded. Twelve patients meeting inclusion criteria declined to participate. Twenty-five women meeting inclusion criteria who received their last expander fill 4 to 8 weeks prior to exchange were enrolled in this cross-sectional study. A patient with a frank Grade IV CC following breast augmentation with a textured implant was included as a positive control ($n = 1$). After randomization and exclusions,[30] power analysis demonstrated that our sample size was sufficient based on the low risk of biofilm formation (1 in 26 patients), or effect size, for the cohort of patients evaluated. At the time of enrollment, clinical history, duration of implantation, device size, style, fill volume, and manufacturer were prospectively recorded. This study meets ethical guidelines for human research conduct and is approved by the Human Research Protection Office at the Washington University in St. Louis School of Medicine (Institutional Review Board # 201101959) and is also registered with clinicaltrials.gov (identification # NCT01060046).

Evaluation of Capsular Contracture

We chose to evaluate CC with both Baker Grade and applanation tonometry as clinically, Baker Grade is widely used to measure capsular contracture while applanation tonometry is used less frequently but may be a more sensitive and reproducible measure.[31,32] On enrollment, these metrics were prospectively recorded for every patient.

Specimen Collection

Biopsies (~2.5 cm^2) were obtained from the submuscular capsule, TE shell, and ADM. A ~1.5 × 0.5 cm segment was collected immediately in an anaerobic transport pack for culture and a 1.0 × 0.5 cm piece was placed in RNA*later* (Sigma Co., St. Louis, MO) to evaluate the transcriptome. Remaining portions of the biopsy were aseptically maintained for live:dead stain, or stored per protocol for H&E staining, quantitative assessment of Type I and III collagen, scanning electron microscopy (SEM), and immunohistochemistry (IHC).[33,34]

EVALUATION FOR BIOFILM

Specimen Culture

Samples of the implant were coated in saline and vortexed for 30 s, while ADM and autologous capsules were minced. The resulting materials were plated on sheep's blood agar, chocolate agar, and pre-reduced Brucella blood agar. The blood and chocolate agar plates were incubated at 35°C in 5% carbon dioxide for 3 days and the Brucella plates incubated for 5 days at 35°C in anaerobic conditions.

PCR Amplification and Sequencing of Bacterial 16S rRNA Genes

Specimens from capsule, breast prosthesis, and ADM stored in RNA*later* were evaluated with real-time quantitative

polymerase chain reactions (qPCR) in all patients (n = 26). Further classification was limited to five randomly selected patients as a result of scant findings with qPCR.[30] Fourteen PCR amplicons, representing all nine 16S variable regions, were constructed using the Fluidigm Access Array System (San Francisco, CA). Five ng/µl of cDNA were input into each reaction. The sample inlets consisted of 1 × High Fidelity FastStart Reaction Buffer without $MgCl_2$, 4.5 nM $MgCl_2$, 5% DMSO (Roche), 200 µM PCR Grade Nucleotide Mix (Roche), 0.05 U/µL FastStart High Fidelity Enzyme Blend (Roche Diagnostics Corporation, Indianapolis, IN) 1 × Access Array Loading Reagent (Fluidigm), 1 µL DNA, and water. The primers were added to the assay inlets at 200 nM forward and reverse primers with 1 × Access Array Loading Reagent. Following PCR amplification, the samples were harvested on the BioMark HD system (Fluidigm). Each sample was harvested and indexed using unique 10 base pair sequences with 14 rounds of PCR to incorporate each index sequence. All samples were pooled into 48 sample libraries and cleaned using bead purification. The samples were loaded on a MiSeq instrument for sequencing (Illumina, San Diego, CA).

Sequencing Data Analysis

Of the 14 PCR amplicons sequenced, only reads from one amplicon that covers the 16S V1 and V2 variable regions were used for downstream analyses. Analysis of the V1-V2 region reads was performed using the QIIME pipeline.[35] Open-reference operational taxonomic units (OTUs) were classified using a custom-built reference database created from 16S sequences contained in the NCBI set of full microbial genomes.[36] Reads were clustered into OTUs by the open source software package Quantitative Insights into Microbial Ecology (QIIME) using the UCLUST clustering algorithm at a threshold of 97% similarity.[37] Representative sequences for each OTU were classified taxonomically using the Ribosomal Database Project (RDP) classifier,[38] using minimum confidence of 80% against the NCBI taxonomy for the custom database. Taxonomy was called to the suborder level. If a given order did not have an annotated suborder then the suborder was set to the order.

CHARACTERIZATION OF CELLULARITY AND COLLAGEN DISTRIBUTION

Several semi-quantitative methods of assessing capsular contracture histologically on the basis of cellularity,[4,9,23,29,39] vascularity,[39,40] fibrosis,[39] or collagen distribution or orientation are reported.[4,9,23,29] However, in the absence of a widely-recognized histologic grading system, we chose to study capsule cellularity and collagen distribution, which have previously been linked to capsular contracture, and about which we have recently reported.[41]

Histopathology: Remodeling Characteristics

Histological preparations from ADM specimens were evaluated based on six remodeling characteristics: cellular infiltration, cell type, host extracellular matrix (ECM) deposition, scaffold degradation, fibrous encapsulation, and neovascularization. The evaluating pathologist, independent of this study, was blinded as to the source and nature of the specimen. A single slide of each specimen was evaluated under light microscopy at 100 × magnification using a previously-reported semi-quantitative scoring system.[42-44] Scores ranged from 0 to 3, with higher scores representing more robust remodeling characteristics. A mean composite remodeling score was calculated from the six component remodeling scores for ADM remodeling. Specimens from the submuscular breast capsule of each patient were evaluated for cellularity, cell type, and vascularity using the same scoring system.

Histopathology: Immunohistochemistry and Fluorescent Imaging

Prior to dehydration, prosthetic ADM and TE specimens from five randomly selected patients were placed in phosphate buffered solution (PBS) and immediately evaluated for viable bacteria using a live:dead stain (Abcam, Cambridge, MA).[30] Samples (0.5 cm^2) were rinsed in 4% PBS, and stained with cell permeable (Ex/Em 488/515 nm) and nonpermeable dyes (Ex/Em 488/615 nm) per manufacturer protocol. When ready for IHC analysis, specimens stored at −80°C were sectioned (~5-10 µm), blocked with 5% normal goat serum and diluted with 0.3% Triton-X in PBS for 1 h. Nuclei were labeled with DAPI and anti-human smooth muscle actin monoclonal antibody using a TRITC-conjugated goat anti-rabbit IgG as the secondary antibody (Life Technologies, Grand Island, NY). Sections were evaluated with an Olympus BX-51 fluorescent microscope and an Olympus FV1000 spectral scanning confocal microscope with a multi-line 458, 488, and 515 nm laser as well as 405 nm, 561 nm, and 633 nm lasers. (Olympus Corporation, Melville, NY).

Histopathology: Collagen Distribution

Sirius Red/Fast Green (SR/FG) stained specimens were prepared and evaluated as we have previously reported to differentiate Type I (red) from Type III (green) collagen.[34,43-45] Slides were photographed under cross-polarized light using an Axioskop 40® microscope and Axiocam® camera (Carl Zeiss®, Thornwood, NY) at 400 × magnification (n = 10 photographs per specimen). Axiovision 4.7® (Zeiss®) software was used to determine the areas (µm^2) occupied by Type I and III collagen and calculate the collagen I:III ratio.

Scanning Electron Microscopy (SEM)

Specimens oriented with methylene blue and a microsuture at the time of biopsy were received in 4% paraformaldehyde and 0.01% glutaraldehyde in Sorensen's buffer. Specimen processing consisted of a rinse in buffer, DDI water, followed by post-fixing in 1% osmium tetroxide for 1 h and dehydration in graded concentrations of ethanol. Specimens were processed in a Tousimis Samdri-780a critical point dryer, and sputter coated with gold-palladium alloy using a Tousimis Samsputter 2a (Rockville, MD). SEM was performed with a Hitachi S2600 (Schaumburg, IL) with 15-20 kV accelerating voltage. Specimens were initially scanned for irregularities at low magnification and then at least five separate locations (all four corners and center) of each specimen were systematically imaged. Areas with heterogeneous morphology were also analyzed.

Statistical Analysis

Mean and standard deviation or median and interquartile range (IQR) were calculated when appropriate based on nature and normality. A two-tailed Wilcoxon signed-rank test or Mann-Whitney U test compared ordinal or non-normally distributed variables between groups. The Chi-square test analyzed differences of race and a two-tailed independent samples *t*-test was used to analyze age differences between the two types of ADM. Alpha was set *a-priori* at 0.05. Statistics were performed using IBM SPSS Statistics version 22 software (Armonk, NY, USA) and were reviewed by an independent biostatistician.

RESULTS

Patient Characteristics

Patients ranging in age from 40 to 64 (49.6 ± 5.5) underwent mastectomy for either cancer prophylaxis or to treat ductal carcinoma *in situ* or a stage Ia invasive ductal carcinoma. Their demographics are summarized in Table 1. All breast prostheses were textured, and the ADM used was Alloderm - Ready to Use (RTU), or Regenerative Tissue Matrix (RTM; LifeCell Corporation, Branchburg, New Jersey). In one case, Seri Scaffold (Allergan; Irvine, CA) biological mesh was used instead of an ADM. Duration of implantation ranged from 91 to 1115 days (Figure 1, Table 2) thus providing sufficient time for biofilm formation.[16,46,47] Baker Grade, applanation tonometry, and duration of implantation by type of ADM are reported in Table 2. Median alloimplant duration was significantly greater for Alloderm RTM than RTU ($P < 0.001$), attributable to the more longstanding availability of the RTM product. Age, race, applanation tonometry score, and Baker Grade did not differ significantly based on alloimplant type.

Table 1. Summary of Patient Characteristics*

Age in years	49.6 ± 5.5 (40-64)
BMI (kg/m^2)	27.0 ± 3.0 (21.9-33.8)
Race	
White	*n* = 18 (69%)
Black	*n* = 6 (23%)
Asian	*n* = 2 (8%)
Duration implanted (days)	172 [141.75, 574.5]
Tissue expander type	
Allergan 133MV	*n* = 20 (80%)
Allergan 133MX	*n* = 5 (20%)
Culture results	*n* = 1 (4%) *Staphylococcus lugdunensis*
	n = 25 (96%) No growth

*Data are reported as Median ± SD (range), Median [Interquartile Range], or *n* (%) as appropriate.

EVALUATION FOR BIOFILM

Molecular and Microbiology

While 77 of 78 cultures from minced and vortexed implant shell, ADM, and capsule biopsies demonstrated no growth, a single tissue expander shell rendered a positive culture for *Staphylococcus luadunensis*.[48] Using bacterial 16S sequencing, the predominant taxa identified was suborder Micrococcineae of class Actinobacteria (Figure 2). Micrococcineae strains are aerobic gram-positive bacteria generally found in soil, sediment, and water environments. The low complexity of the samples and the fact that Micrococcineae is naturally found on the human skin suggests that the MiSeq reads were from contaminates.

Scanning Electron Microscopy

No evidence of biofilm formation was noted in 25 of 26 patients evaluated with SEM (Figure 3). Textured TEs demonstrate morphology consistent with *Biocell*® technology (Figure 3A). While regions of the textured surface were covered with an amorphous, lobulated substance, their size was not consistent with bacteria (Figure 3B). Submuscular biopsies were devoid of biofilms (Figure 3C), but it is feasible that some of these spheres are consistent with sporadic cocci (Figure 3D). ADMs were characterized by strands of collagen with variable thickness and orientation (Figure 3E),

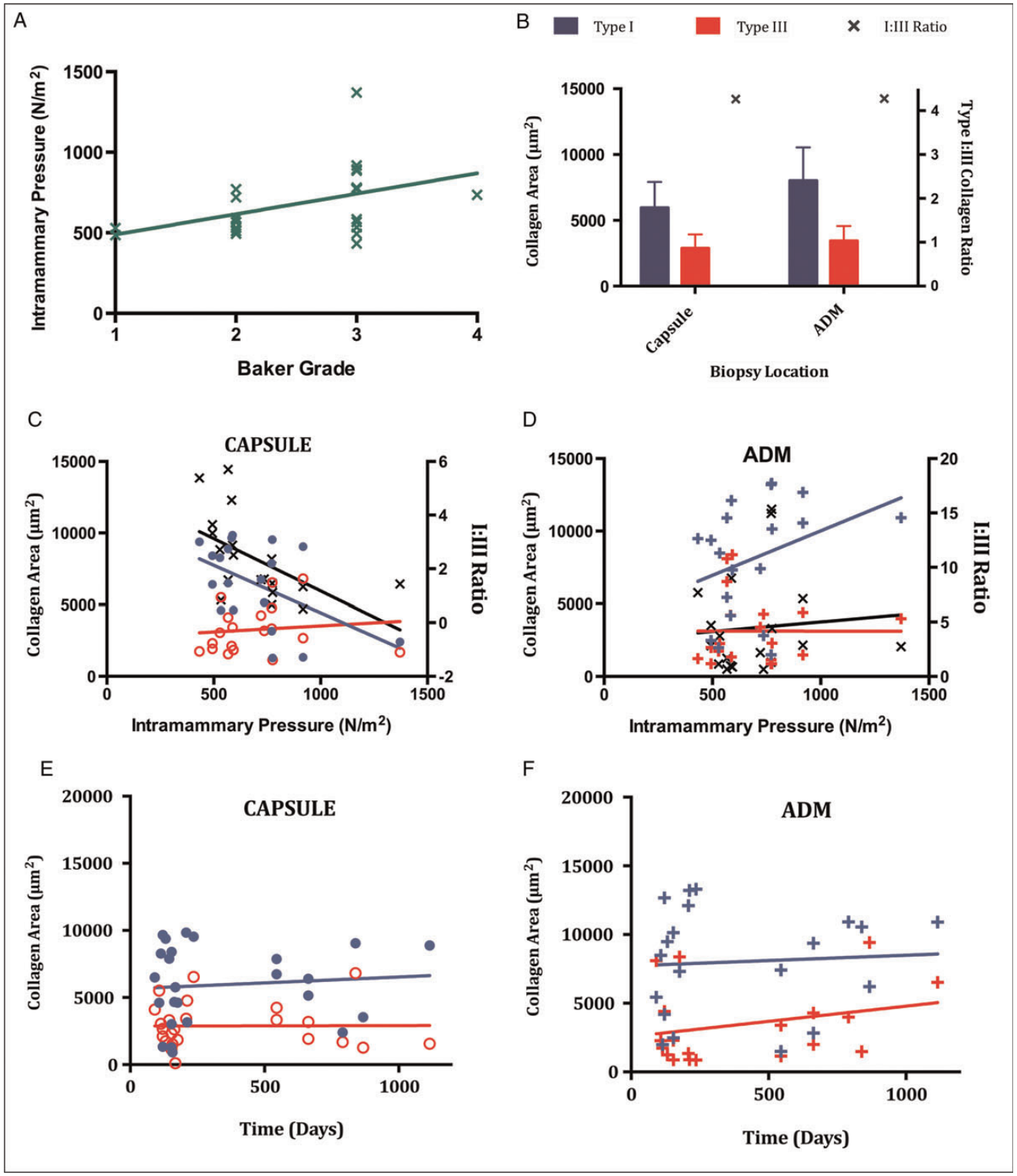

Figure 1. (A) Baker Grade (1 to 4) was assessed utilizing the modification published by Spear for breast reconstruction,[31] and was correlated with applanation tonometry used to calculate intramammary pressure (N/m^2).[32] Intramammary pressure (green "x") is plotted against clinical Baker Grade. (B) Pooled mean Type I and III collagen values and I:III collagen ratio. Type I collagen is blue, Type III collagen is red, and "x" represents the I:III collagen ratio. (C) Capsular Type I and III collagen as a function of intramammary pressure. (D) ADM Type I and III collagen as a function of intramammary pressure. (E) Capsular Type I and III collagen area versus duration of implantation. (F) ADM Type I and III collagen area versus duration of implantation. Each data point is derived from a mean of values from 10 sample fields taken from the same biopsy specimen. Type I collagen in capsule (filled blue circle), Type I collagen in ADM (blue " + "), Type III collagen in capsule (empty red circle), Type III collagen in ADM (red " + "), I:III collagen ratio (black "x"). Straight lines represent best-fit linear regression plots for variables including Type I collagen (blue line), Type III collagen (red line), and ratio (black line).

Table 2. Patient Characteristics by Alloimplant Type[a]

	Alloderm (RTU)	Alloderm (RTM)	Seri Surgical Scaffold	*P*-value
Number of patients	16 (64%)	8 (32%)	1 (4%)	_
Age	49.13 ± 5.22	51.88 ± 6.27	46	0.23
Race				0.441
White	10 (63%)	6 (75%)	1 (100%)	
Black	4 (25%)	2 (25%)		
Other	2 (12%)			
Implant duration (days)	154 [121, 208]	663 [545, 791]	153	**<0.001**
Applanation tonometry (N/m^2)	567 [510, 780]	733.5 [721, 774]	775	0.130
Baker grade	3 [2, 3]	3 [2, 3]	3	0.336

[a]Data are reported as Median [Interquartile Range], or *n* (%) as appropriate. $P < 0.05$ statistically significant.

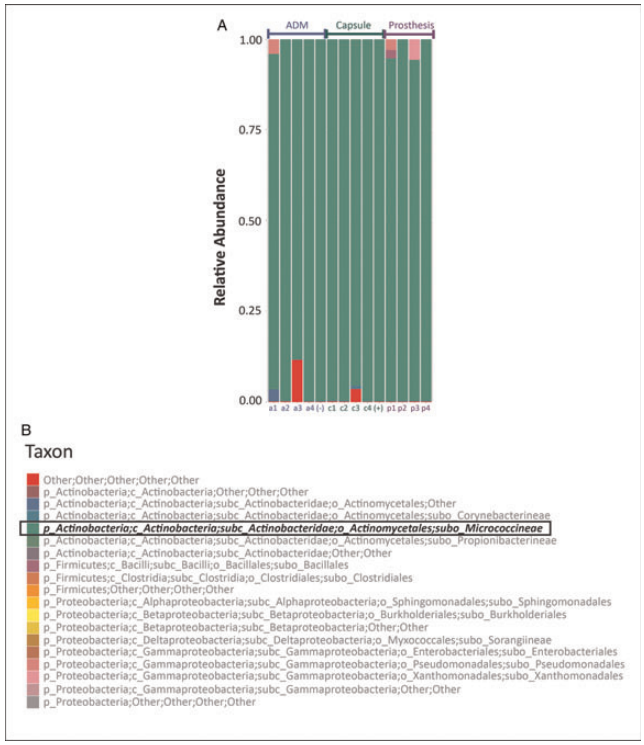

Figure 2. The relative abundance of each bacterial taxa in all sequenced samples color-coded by cluster (A). In all samples the majority taxa was suborder Micrococcineae of class Actinobacteria colored green (B). Samples from five patients are shown. Patients 1 through 4 contributed samples of ADM (a1-a4), capsule (c1-c4), and prosthesis (p1-p4). A frank CC specimen contains prosthesis and capsule together and serves as positive control (+). A fifth piece of nonimplanted Alloderm RTU served as a negative control piece of ADM (–).

and infrequently, with sparse spheres that may represent persistent bacteria (Figure 3F).

Morphologic evidence suggestive of biofilm formation was noted in specimens derived from a single patient with Baker Grade III capsule, an intramammary pressure of 777 N/m^2, and negative cultures (Figure 4). Spheres whose size and morphology were consistent with cocci appeared to congregate on both the capsule (Figure 4C and D) and ADM (Figure 4E and F) of this specimen. We did not identify any structures consistent with bacteria on the surface of this TE. A patient with a severe, Baker Grade 4 CC, 13 years following primary aesthetic breast augmentation, presented with an intramammary pressure of 945 N/m^2 and negative cultures. SEM demonstrated collagen fibers of variable orientation, thickness, and density as well as both lymphocytes and macrophages, but no obvious biofilm in this positive control (Figure 5).

CHARACTERIZATION OF CELLULARITY AND COLLAGEN DISTRIBUTION

Light, Fluorescent, and Confocal Microscopy

Cell type, cellularity, and vascularity scores of capsular and ADM samples are reported in Table 3. Cellular infiltration scores were significantly greater in capsules ($P < 0.05$), but there were no differences in cell type or vascularity. Intramammary pressure increased significantly ($P = 0.026$) with Baker Grade (Figure 1A).

Type I collagen and the I:III ratio decreased with an increase in intramammary pressure in capsular tissue (Figure 1C) but not within the ADM (Figure 1D). Type I and III collagen content remained relatively stable in specimens biopsied at both early and late time points (Figures 1E and F, 3C and D), and the mean ratio of type I:III collagen remained the same (4.3:1) in biopsies harvested from the submuscular capsule and the ADM (Figures 1B, and 6C and D). Mean collagen content was higher overall in biopsied ADM than capsular specimens.

Live:dead stain failed to identify any viable cells in the processed prosthetic specimens ($n = 5$). Immunohistochemistry confirmed the presence of myofibroblasts within all evaluated capsules ($n = 10$). Qualitatively, DAPI-stained nuclei were densely distributed in capsular tissue, and less densely distributed in ADMs, with no staining on the breast implant surface. Semi-quantitative evaluation of H&E-stained biopsies from the capsule

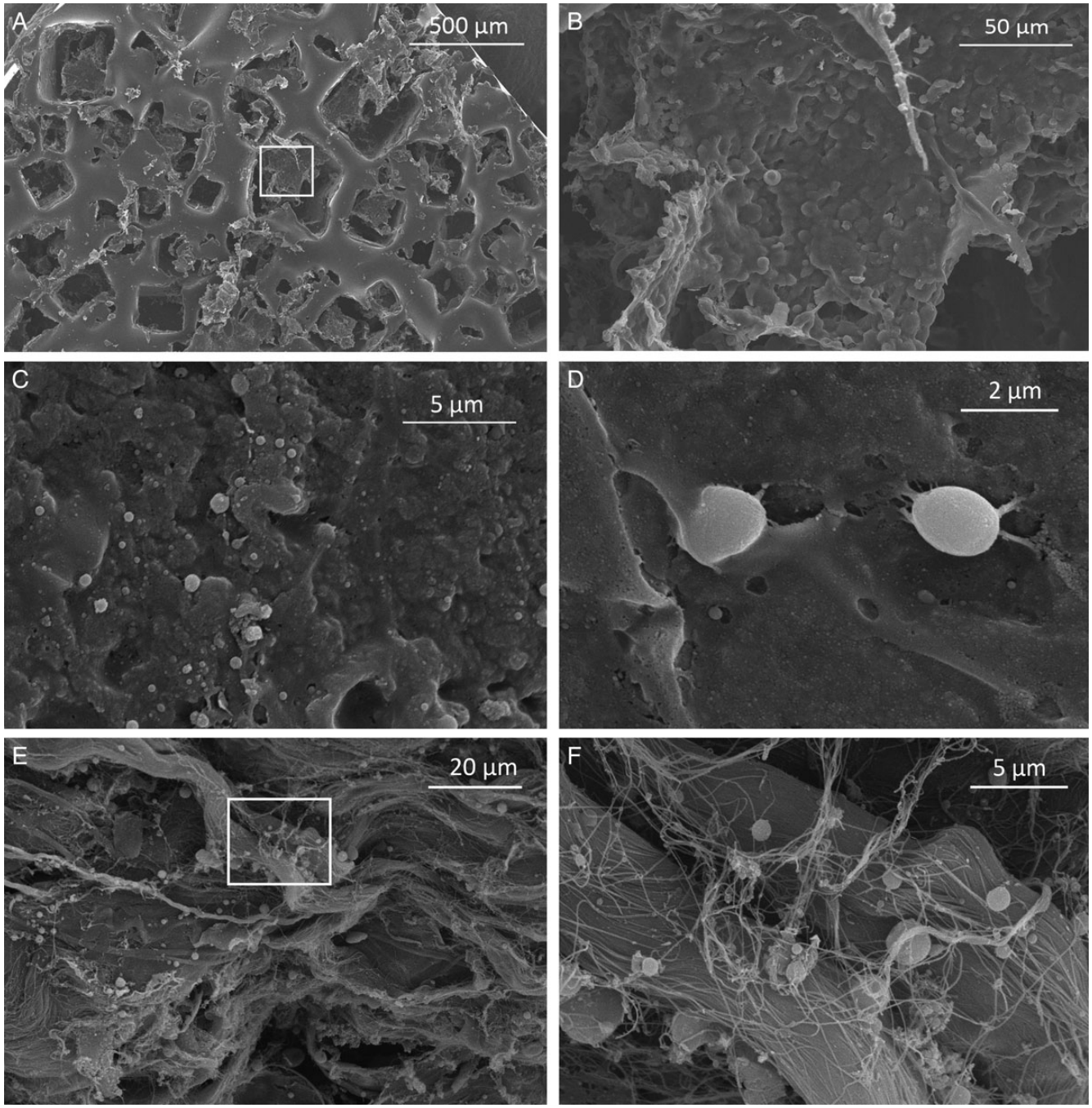

Figure 3. Representative scanning electron micrographs. (A) Textured surface (*Biocell*®) of an Allergan 133MV tissue expander (50 × magnification). Panel B magnifies the contents of the white box. (B) Magnified view of amorphous material over surface of prosthesis. There is no evidence of structures whose size or morphology resemble bacteria (500 × magnification). (C) Submuscular capsule devoid of biofilms (5000x magnification). (D) A ~2 µm sphere appears to be adherent to submuscular capsule. This structure is smaller than a blood cell but larger than a typical bacteria (10,10,000 × magnification). (E) ADM (Alloderm RTM) with numerous bundles of collagen. Panel F magnifies the contents of the white box (1000 × mag). (F) with a few spheres < 1 µm, but no discrete biofilm (5000 × magnification).

(Figure 6A) and ADM (Figure 6B) revealed collagen distributed in an organized fashion (Figure 6C and D) with 100 to 150 cells and 6 to 10 blood vessels per high-powered field (Table 3).

DISCUSSION

Our results show no correlation between biofilm formation and CC. This discrepancy may relate to how CC is defined,

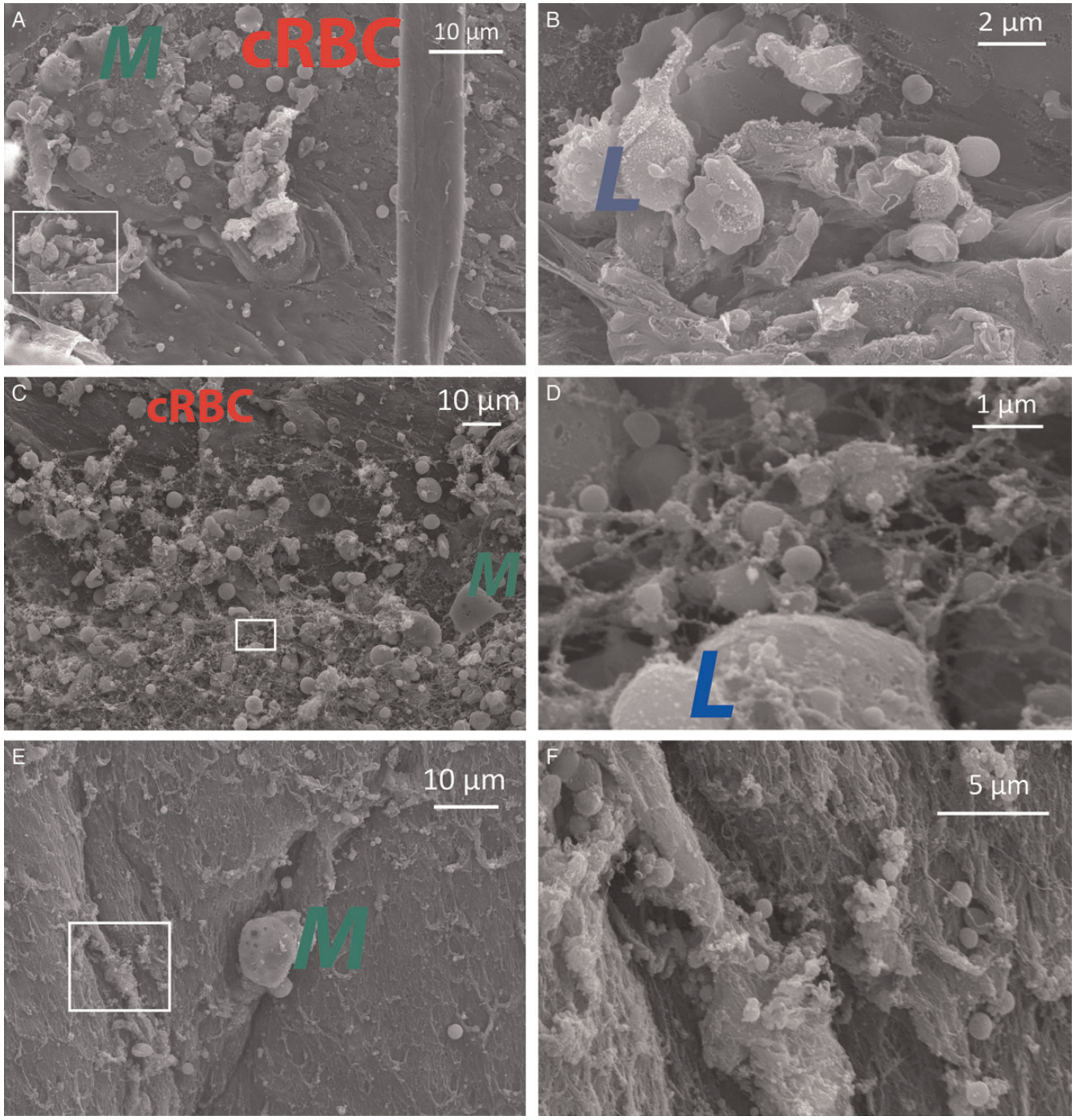

Figure 4. Scanning electron microscopy strongly suggested biofilm formation in capsular, ADM, and prosthetic biopsies obtained from one patient. This patient had a Baker Grade III capsule, intramammary pressure of 777 N/m^2, and negative cultures. (A) Submuscular capsule specimen demonstrates several macrophages (M) and crenated erythrocytes (cRBC) (1000 × magnification). Panel B magnifies the contents of the white inset box. (B) Magnified inset shows lymphocytes (L) (5000 × magnification). (C) Submuscular capsule with macrophages (M) and crenated erythrocytes (cRBC). Panel D magnifies the contents of the white inset box (1000 × magnification). (D) At increased magnification, several spheres whose sizes (< 1 µm) are consistent with cocci are apparent as well as a larger lymphocyte (L). These are interconnected by strands of material whose appearance may represent extracellular biofilm matrix (15,000 × magnification). (E) ADM (Alloderm RTU) demonstrates a more uniform morphology disrupted by focal areas of heterogeneity including a macrophage (M). Panel F magnifies the contents of the white inset box (1000 × magnification). (F) Magnified inset demonstrates focal areas where cocci appear to congregate. Early biofilm formation is feasible in this region. No bacteria where identified on the surface of the prosthesis in this subject. PCR demonstrated scant Micrococcineae in this specimen (5000 × magnification).

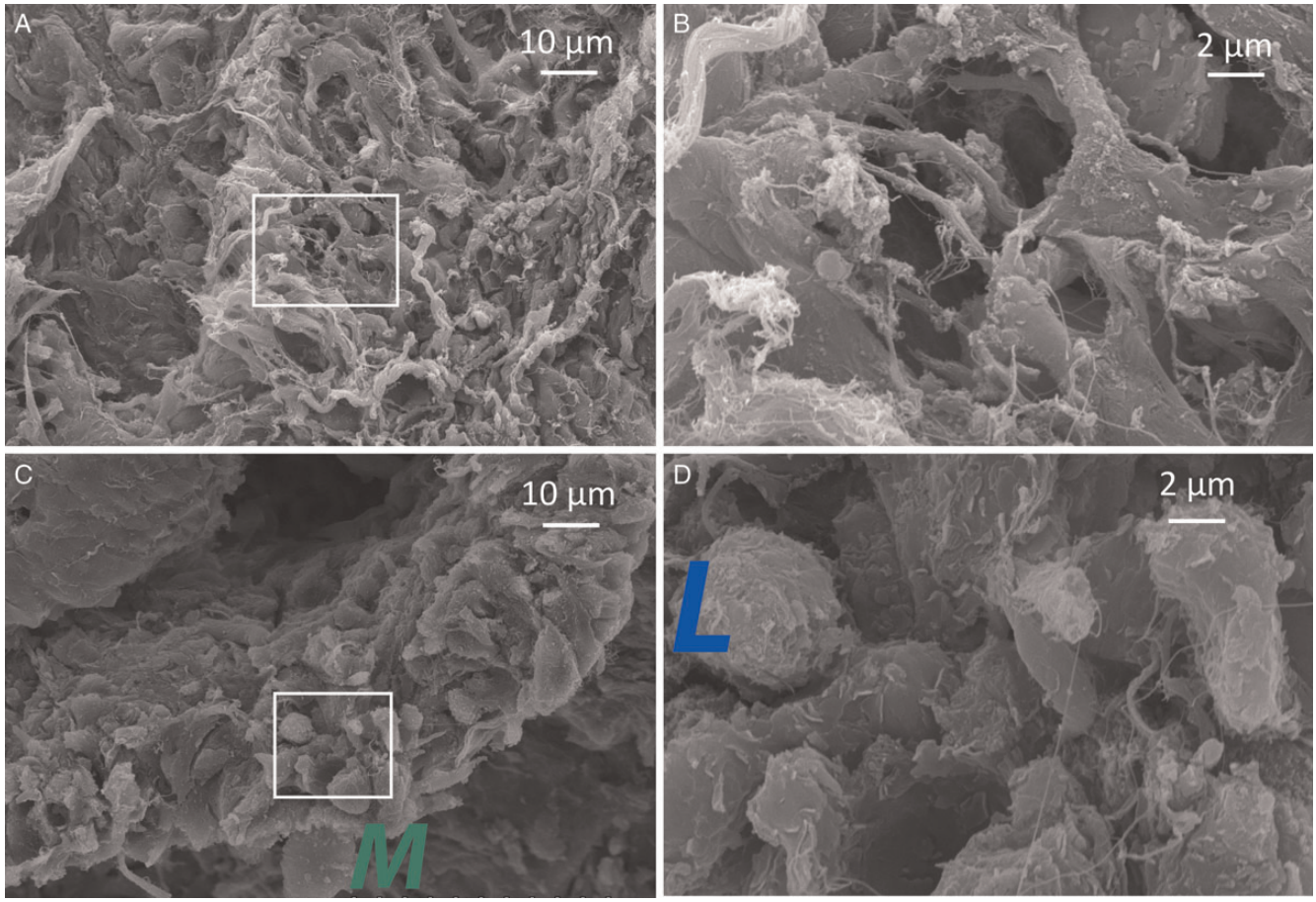

Figure 5. Scanning electron microscopy of a patient with clinically frank (Baker Grade IV) CC 13 years following breast augmentation. (A) Randomly distributed collagen bundles of variable thickness are identified (1000 × magnification). Panel B magnifies the contents of the white inset box. (B) No biofilm, bacterial remnant, or individual bacteria noted at 5000 × magnification. (C) Thickened capsular specimen devoid of obvious bacteria, notable for structures whose morphology and size are consistent with macrophages (M) (1000 × magnification) and (D) with magnification, lymphocytes (L) (5000 × magnification).

which in most studies, involves Baker Grade, applanation tonometry, or the breast augmentation classification.[49-53] These metrics, however, are influenced not only by CC, but also the unique density and volume of the prosthesis, and the elasticity and surface area of the surrounding soft tissue envelope. For example, in two patients with histologically identical capsules, the one with pre-existing glandular ptosis who receives only a breast augmentation with a moderate profile saline implant will have a lower intramammary pressure compared to a patient with dense breasts who receives a high projecting cohesive gel implant with concomitant mastopexy. In this case, with the same capsule histologically, one may be a Baker 1 and the other a Baker 3. Baker Grade and applanation tonometry are still extremely useful, particularly when repeat measures of intramammary pressure are serially applied to the same breast in a longitudinal study design. However, in a cross-sectional study design when different breasts are compared to each other, additional variables are introduced that impact breast "firmness" that may or may not be the result of changes to the capsule itself. While Baker Grade in particular was not originally intended to evaluate the periprosthetic capsule around tissue expanders, we utilized this scale along with applanation tonometry in the absence of a more specific clinical grading system and also supplemented this recognized deficiency with a robust histologic analysis. The unintended widespread use of Baker Grade as a ubiquitous, subjective method to analyze capsular contracture is recognized, and its adaptation for classifying prosthetic breast reconstruction has been reported.[31] More robust techniques for evaluating capsular contracture including clinical assessment with ultrasound elastography,[54] computed tomography,[55] or histologically have been described,[2,9,29,39,56-58] but have yet to be widely adopted.

In our study, the presence of isolated cocci on SEM and the identification of the bacterial subclass Micrococcineae on bacterial taxonomy (Figure 2) suggest either sample contamination or the presence of persister cells. A dense

Table 3. Histologic Grading of Submuscular Capsule and ADM Remodeling

Histologic Criteria	Submuscular Capsule Median [IQR]	ADM Remodeling Median [IQR]	*P*-value
Cell type	2.00 [2.00, 3.00]	2.25 [2.00, 3.00]	0.314
Cellular infiltration	3.00 [3.00, 3.00]	3.00 [2.00, 3.00]	**<0.02**
ECM deposition		2.92 [2.00, 3.00]	
Scaffold degradation		2.19 [1.00, 3.00]	
Fibrous encapsulation		2.88 ± [2.00, 3.00]	
Neovascularization	3.00 [3.00, 3.00]	3.00 [2.88, 3.00]	0.286
Mean composite		2.64 ± [2.00, 3.00]	

P < 0.05 statistically significant.

population of bacteria in a biofilm will use quorum sensing to regulate gene expression and modulate virulence and antibiotic expression.[59,60] Persister cells existing in or out of a biofilm are nonreplicating, possess intracellular mechanisms immune to antibiotic corruption,[61] and require complex strategies to eradicate.[62-64] The concentration and distribution of both persister cells and biofilms is dynamic.[65] It is possible that biofilms escaped detection in our study because at the time of biopsy, causative organisms existed as antibiotic-tolerant persister cells with the capacity to form latent biofilms. Persister cells may also provide a mechanism by which biofilms can ultimately migrate to involve more widespread areas of the prosthesis surface and its adjacent capsule.

We studied the TE/I exchange paradigm to obtain a large number of human specimens from the submuscular capsule, ADM, and prosthesis at multiple time points post-implantation. Based on previous work, we anticipated

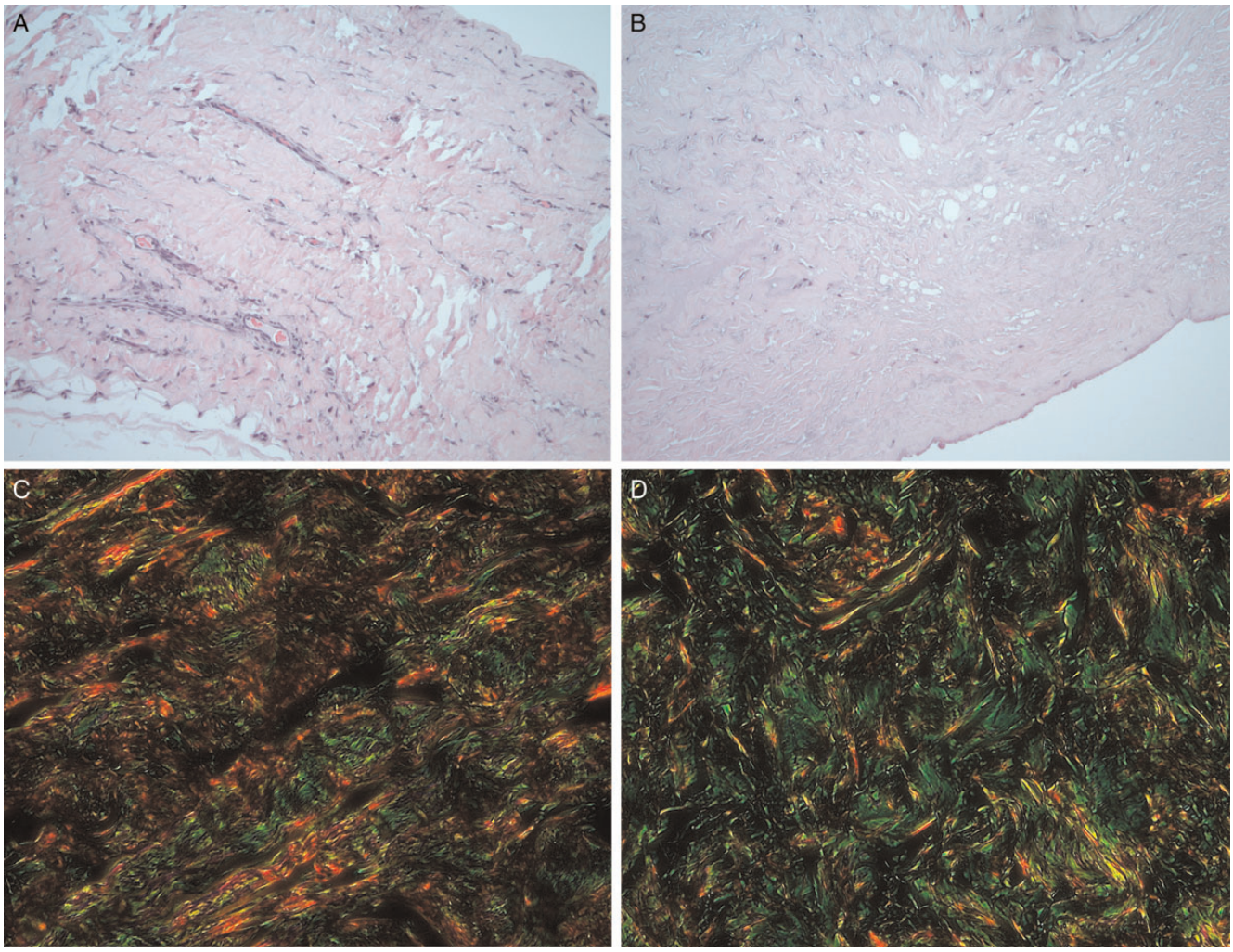

Figure 6. Representative samples stained with H&E biopsied from (A). Submuscular capsule and (B) ADM. To assess collagen, samples from the (C) submuscular capsule and (D) ADM were labeled with Sirius Red (Type I collagen) and Fast Green (Type III collagen).

Table 4. Focused Review of Methods Studies Have Used to Examine an Association Between Subclinical Infection and Capsular Contracture

Study	Implant Host	Sample Size	Duration of Implantation	Clinical Method for Evaluating Capsule	Histologic Method for Evaluating Capsule	Culture Method	IHC[a]/Light Microscopy	SEM[b]	Molecular Biology
Pajkos et al[15]	Human	27 breasts, 19 Baker III/IV	0.4 to 26 years (mean 9.2 years)	Baker Grade	No	Sonication, broth	No	Yes	No
Jacombs et al[14]	Swine	121 breasts	19 wks	Baker Grade	No	Sonication, broth	Live:Dead stain	Yes	rtPCR, genomic DNA
Rieger et al[19]	Human	121 breasts	Augmentation: Mean 4.0 years (0.1 to 32); Reconstruction: Mean 3.0 months (1 to 6)	Baker Grade	No	Sonication, broth	No	No	No
Tamboto et al[16]	Swine	51 breasts	13 weeks	Baker Grade	No	Sonication, broth	No	Yes	No
Allan et al[13]	Swine/Human	6 swine implants; 1 human implant	20 weeks (swine); rapidly developing Grade III (human)	Baker Grade	No	Sonication, broth	No	Yes	*Ica* gene evaluation
Jacombs et al[14]	Swine	28 breasts	16 weeks	Applanation Tonometry + Baker Grade	Contracted capsule had greater volume and mass and reduced surface area	Sonication, broth & PCR-based bacterial viability	No	Yes	Yes
Adams et al[22]	Human	330 breasts aesthetic augmentation; 44 breasts augmentation-mastopexy; 99 breasts reconstructions	6 to 75 months	Baker Grade	No	Impact of antibiotic pocket irrigation study	No	No	No
Giordano et al[20]	Human	660 breasts (aesthetic augmentation through IMF incision)	24 ± 13 months (no pocket irrigation); 22 ± 3 months (pocket irrigation)	"Modified" Baker Grade	No	Impact of antibiotic pocket irrigation study	No	No	No
Marques et al[29]	Rabbit	31 rabbits	4 weeks	Intracapsular Pressure of Implant + Baker Grade	Yes	Incubation in broth	No bacterial assessment. Capsule assessed.	No	No
Rieger et al[75]	Human	13 patients; 22 breasts	10.4 years (0.25 to 30)	Baker Grade	No	Sonication, agar plates	No	No	No
Bergmann et al[58]	Rat	80 breasts	60 days	No	Yes	Sonication, broth	No bacterial assessment. Capsule assessed.	No	No
Del Pozo[77]	Human	45 breasts	(+)Cap Con 16.4 (0.65-33.87) years (–)Cap Con 14.8 (0.46-24.49) years	Baker Grade	No	Sonication, agar plates	No	No	No

[a]IHC: immunohistochemistry. [b]SEM: scanning electron microscopy.

identifying more biofilms than we found,[66] particularly noting our use of textured expanders.[18,66] Low bacterial yield resulting from our chosen methodologies or sampling bias may explain missing biofilms by SEM since $<0.1\%$ of the surface was imaged in this study. Previous evaluation of craniofacial miniplates,[67] or breast implants in swine,[16] assessed surface areas that were several orders of magnitude smaller, significantly reducing the impact of sampling bias. If biofilms were present in these capsules and they were simply missed due to sampling bias, it would suggest that bacteria may only require a sporadic or heterogeneous interaction with the capsule either physically or temporally to elicit a contracture.[16,67]

Some evidence has suggested that bacterial biofilms are a component of "the principal pathogenic pathway to development of CC".[13-15,17-19,21,58,66,68-77] Indirect evidence demonstrated lower CC rates with periprosthetic delivery of antibiotics via irrigation[20,22] or an impregnated mesh.[14] Deliberate inoculation of the periprosthetic pocket with bacteria leads to CC in animal models.[14,16,18] In this study, however, specimens from only one of 26 patients demonstrated evidence of a microbial biofilm.

Confirming the presence of a biofilm—"a structured community of bacterial cells enclosed in a self-produced polymeric matrix and adherent to an inert or living surface"[78]—is challenging and cost-prohibitive for routine clinical practice. A multimodality or "full circle" approach originally described by Amann et al[79] represents a more complete approach that includes imaging with electron or confocal microscopy to demonstrate "growth in place"[80] of a biofilm morphologically,[67,80-84] and verification of the presence, viability, and species of bacteria with techniques like PCR, coupled PCR-mass spectrometric (PCR-MS) assay,[83,85] or fluorescent-in situ hybridization (FISH).[83,85,86] Bacterial genomic DNA amplification techniques are extremely sensitive, but not specific for a biofilm since individual and even nonviable bacteria render a positive result. Sophisticated imaging techniques to identify bacterial biofilms have been reported in other clinical implantable device paradigms,[67,87,88] but are limited (Table 4) in the human CC literature.[13,15,17] Moreover, studies reporting the use of PCR or a live:dead stain to identify bacterial biofilms on breast implants are currently limited to studies in animal models.[13,14,18] Sonication has been effectively utilized by many investigators to dislodge bacteria from a biofilm to increase the sensitivity of bacterial culture.[19,75] By its very mechanism of action, however, sonication disrupts and converts biofilm-derived bacteria to a planktonic form and precludes confirmation of their biofilm origin with subsequent direct imaging techniques. Under optimized experimental conditions,[89] sonication is an important adjunct to bacterial culture with widespread utility.[19,75] However, PCR—as we have employed—is a more sensitive diagnostic modality,[81,90,91] and reports that sonication can damage or alter bacterial growth remain.[89,92] Since biofilms are not visually confirmed, the source of bacteria cultured following sonication, or evaluated with PCR, may include a biofilm or planktonic bacteria derived from the prosthesis or an environmental contaminate.[81,92,93] In our study, it is feasible that relative to sonication, vortexing less effectively dislodged bacteria from the prosthesis, ADM, or capsule and reduced the sensitivity of our cultures. For this reason, we also used real-time PCR to increase the sensitivity of our detection, classify bacteria (Figure 2), and with the aid of live:dead stain, confirm viability. However, even if all of these other assays were positive, including implementation of sonication, in the absence of their direct visualization in a colony (Figures 3-5) the presence of biofilms still could not have been confirmed.

A causative relationship between biofilm formation and CC is difficult to prove.[20] Bacteria can initiate an upstream inflammatory reaction by elaborating toxins or inciting an immune response, which may lead to fibrosis and CC.[3] Whether biofilms impact the capsule locally or can influence remote capsular tissue with which they are not in contact is unknown. The species, concentration, and environmental triggers that cause a bacterial biofilm to trigger a CC rather than an unrelated immune response have not been described.[1] Bacteria may form biofilms as a survival mechanism to ensure viability when exposed to hostile proinflammatory environments. It is therefore possible that stressful stimuli independently lead to both a biofilm and inflammation, rather than the biofilm causing the inflammation. Strong evidence shows that antimicrobial therapy *induces* biofilm formation in some clinical paradigms to confer resistance.[94-96] Contrary to evidence favoring antibiotic pocket irrigation to attenuate CC rates,[20,22] recent cohort studies comparing triple antibiotic to saline irrigation demonstrate no difference in CC rates.[94,97,98] Elucidating a relationship between biofilm formation and CC merits further study.

ADMs may be more prone to biofilm formation as they are associated with more bacterial adhesion than proline or vicryl mesh.[99] Still, ADMs remain a reported strategy to reduce the contractile properties of the periprosthetic pocket,[26] and our study identified too few biofilms to reliably identify a relationship between biofilms, ADMs, and CC.

CONCLUSION

Our study does not refute an association between biofilms and CC. Rather, it shows that in a clinical setting, identifying a biofilm with multimodality methodology that includes direct imaging is challenging where sampling of a relatively large surface area may be prohibitive. Identification of a molecular mechanism by which potentially proinflammatory etiologies such as bacteria actually trigger contracture histopathologically is also required. Finally, it underscores the need for more specific clinical and histologic methodologies to differentiate capsular pathology from characteristics of the prosthesis or noncapsular soft tissue envelope that may also be influencing breast compliance. Modern advances in molecular biology and imaging continue to provide better tools to develop a more sophisticated understanding and characterization of CC.

Acknowledgements

We are very grateful to the Aesthetic Surgery Education Research Foundation, whose generous grant to Dr Myckatyn supported this study. The authors are also grateful to Dr Carey-Ann Burnham (Medical Director, Clinical Microbiology

at the Washington University School of Medicine) for her expertise regarding cultures derived from breast implant and ADM prostheses. We are also grateful to Dr Andres Roma (Department of Anatomic Pathology, Cleveland Clinic, Cleveland, Ohio) for histologic grading of H&E stained biopsies of capsules and ADMs, and Ms. Piyaraj Newton (Division of Plastic and Reconstructive Surgery Research Laboratory, Washington University School of Medicine) for assistance with immunohistochemistry. We thank the Genome Technology Access Center in the Department of Genetics at Washington University School of Medicine for help with genomic analysis. The Center is partially supported by a NCI Cancer Center Support Grant (#P30 CA91842) to the Siteman Cancer Center and by an ICTS/CTSA Grant (# UL1TR000448) from the National Center for Research Resources (NCRR), a component of the National Institutes of Health (NIH), and NIH Roadmap for Medical Research. Scanning electron microscopy was performed by Jaclynn Lett, Senior Research Technician in the Electron Microscopy Facility within the Research Center for Auditory and Vestibular Studies at Washington University School of Medicine. This facility is supported by the National Institutes of Health NIDCD Grant P30DC04665. This publication is solely the responsibility of the authors and does not necessarily represent the official view of NCRR or NIH.

Disclosures

Dr Myckatyn receives consulting, speaker, and research grant fees from LifeCell (Bridgewater, NJ) and Allergan (Irvine, CA), and consulting fees from Andrew Technologies (Wheeling, IL). Products from Allergan (breast prostheses) and LifeCell (acellular dermal matrices) were used in this study, but there was no industry funding or involvement with this study. Dr Tenenbaum receives consulting fees from Seintra (Santa Barbara, CA) and Andrew Technologies (Wheeling, IL). No products from these companies were used in this study. None of the other authors have anything to disclose.

Funding

This study was supported by a grant from the Aesthetic Surgery Education and Research Foundation to Dr Terence Myckatyn. These funds were used exclusively for specimen processing, laboratory costs, and assistance with statistical analysis.

REFERENCES

1. Adams WP Jr. Capsular contracture: what is it? What causes it? How can it be prevented and managed? *Clinics in Plastic Surgery*. 2009;36(1):119-126, vii.
2. Moyer KE, Ehrlich HP. Capsular contracture after breast reconstruction: collagen fiber orientation and organization. *Plastic and Reconstructive Surgery*. 2013;131(4):680-685.
3. Katzel EB, Koltz PF, Tierney R, et al. The impact of Smad3 loss of function on TGF-beta signaling and radiation-induced capsular contracture. *Plastic and Reconstructive Surgery*. 2011;127(6):2263-2269.
4. Marques M, Brown SA, Cordeiro ND, et al. Effects of fibrin, thrombin, and blood on breast capsule formation in a preclinical model. *Aesthet Surg J*. 2011;31(3):302-309.
5. Tan KT, Baildam AD, Juma A, Milner CM, Day AJ, Bayat A. Hyaluronan, TSG-6, and inter-alpha-inhibitor in periprosthetic breast capsules: reduced levels of free hyaluronan and TSG-6 expression in contracted capsules. *Aesthet Surg J*. 2011;31(1):47-55.
6. San-Martin A, Dotor J, Martinez F, Hontanilla B. Effect of the inhibitor peptide of the transforming growth factor beta (p144) in a new silicone pericapsular fibrotic model in pigs. *Aesthetic Plastic Surgery*. 2010;34(4):430-437.
7. Zimman OA, Toblli J, Stella I, Ferder M, Ferder L, Inserra F. The effects of angiotensin-converting-enzyme inhibitors on the fibrous envelope around mammary implants. *Plastic and Reconstructive Surgery*. 2007;120(7):2025-2033.
8. D'Andrea F, Nicoletti GF, Grella E, et al. Modification of cysteinyl leukotriene receptor expression in capsular contracture: Preliminary results. *Annals of Plastic Surgery*. 2007;58(2):212-214.
9. Wolfram D, Rainer C, Niederegger H, Piza H, Wick G. Cellular and molecular composition of fibrous capsules formed around silicone breast implants with special focus on local immune reactions. *Journal of Autoimmunity*. 2004;23(1):81-91.
10. Siggelkow W, Faridi A, Spiritus K, Klinge U, Rath W, Klosterhalfen B. Histological analysis of silicone breast implant capsules and correlation with capsular contracture. *Biomaterials*. 2003;24(6):1101-1109.
11. Bastos EM, Neto MS, Alves MT, et al. Histologic analysis of zafirlukast's effect on capsule formation around silicone implants. *Aesthetic Plastic Surgery*. 2007;31(5):559-565.
12. Grella E, Grella R, Siniscalco D, et al. Modification of cysteinyl leukotriene receptors expression in capsular contracture: follow-up study and definitive results. *Annals of Plastic Surgery*. 2009;63(2):206-208.
13. Allan JM, Jacombs AS, Hu H, Merten SL, Deva AK. Detection of bacterial biofilm in double capsule surrounding mammary implants: findings in human and porcine breast augmentation. *Plastic and Reconstructive Surgery*. 2012;129(3):578e-580e.
14. Jacombs A, Allan J, Hu H, et al. Prevention of biofilm-induced capsular contracture with antibiotic-impregnated mesh in a porcine model. *Aesthet Surg J*. 2012;32(7):886-891.
15. Pajkos A, Deva AK, Vickery K, Cope C, Chang L, Cossart YE. Detection of subclinical infection in significant breast implant capsules. *Plastic and Reconstructive Surgery*. 2003;111(5):1605-1611.
16. Tamboto H, Vickery K, Deva AK. Subclinical (biofilm) infection causes capsular contracture in a porcine model following augmentation mammaplasty. *Plastic and Reconstructive Surgery*. 2010;126(3):835-842.
17. Deva A, Chang LC. Bacterial biofilms: a cause for accelerated capsular contracture? *Aesthet Surg J*. 1999;19(2):130-133.
18. Jacombs A, Tahir S, Hu H, et al. In vitro and in vivo investigation of the influence of implant surface on the formation of bacterial biofilm in mammary implants. *Plastic and Reconstructive Surgery*. 2014;133(4):471e-480e.

19. Rieger UM, Mesina J, Kalbermatten DF, et al. Bacterial biofilms and capsular contracture in patients with breast implants. *The British Journal of Surgery*. 2013;100 (6):768-774.
20. Giordano S, Peltoniemi H, Lilius P, Salmi A. Povidone-iodine combined with antibiotic topical irrigation to reduce capsular contracture in cosmetic breast augmentation: a comparative study. *Aesthet Surg J*. 2013;33(5):675-680.
21. van Heerden J, Turner M, Hoffmann D, Moolman J. Antimicrobial coating agents: can biofilm formation on a breast implant be prevented? *Journal of Plastic, Reconstructive & Aesthetic Surgery: JPRAS*. 2009;62(5):610-617.
22. Adams WP Jr., Rios JL, Smith SJ. Enhancing patient outcomes in aesthetic and reconstructive breast surgery using triple antibiotic breast irrigation: six-year prospective clinical study. *Plastic and Reconstructive Surgery*. 2006;118:(7 Suppl):46S-52S.
23. Marques M, Brown SA, Rodrigues-Pereira P, et al. Animal model of implant capsular contracture: effects of chitosan. *Aesthet Surg J*. 2011;31(5):540-550.
24. Salzberg CA, Ashikari AY, Koch RM, Chabner-Thompson E. An 8-year experience of direct-to-implant immediate breast reconstruction using human acellular dermal matrix (AlloDerm). *Plastic and Reconstructive Surgery*. 2011;127(2):514-524.
25. Maxwell GP, Gabriel A. Use of the acellular dermal matrix in revisionary aesthetic breast surgery. *Aesthet Surg J*. 2009;29(6):485-493.
26. Namnoum JD, Moyer HR. The role of acellular dermal matrix in the treatment of capsular contracture. *Clinics in plastic surgery*. 2012;39(2):127-136.
27. Stump A, Holton LH 3rd, Connor J, Harper JR, Slezak S, Silverman RP. The use of acellular dermal matrix to prevent capsule formation around implants in a primate model. *Plastic and Reconstructive Surgery*. 2009;124 (1):82-91.
28. Basu CB, Leong M, Hicks MJ. Acellular cadaveric dermis decreases the inflammatory response in capsule formation in reconstructive breast surgery. *Plastic and Reconstructive Surgery*. 2010;126(6):1842-1847.
29. Marques M, Brown SA, Cordeiro ND, et al. Effects of coagulase-negative staphylococci and fibrin on breast capsule formation in a rabbit model. *Aesthet Surg J*. 2011;31(4):420-428.
30. Urbaniak GC, Plous S. Research Randomizer *[computer program]*. Version 4.02013.
31. Spear SL, Baker JL Jr. Classification of capsular contracture after prosthetic breast reconstruction. *Plastic and Reconstructive Surgery*. 1995;96(5):1119-1123. discussion 1124.
32. Moore JR. Applanation tonometry of breasts. *Plastic and Reconstructive Surgery*. 1979;63(1):9-12.
33. Hunter DA, Moradzadeh A, Whitlock EL, et al. Binary imaging analysis for comprehensive quantitative histomorphometry of peripheral nerve. *Journal of Neuroscience Methods*. 2007;166(1):116-124.
34. Cavallo JA, Gangopadhyay N, Dudas J, et al. Remodeling Characteristics and collagen distribution of biologic scaffold materials biopsied from postmastectomy breast reconstruction sites. *Ann Plast Surg*. 2015;75(1):74–83.
35. Caporaso JG, Kuczynski J, Stombaugh J, et al. QIIME allows analysis of high-throughput community sequencing data. *Nature Methods*. 2010;7(5):335-336.
36. NCBI. Full Microbial Genomes 2013. ftp://ftp.ncbi.nlm.nih.gov/genomes/Bacteria/. Accessed 2 Sept. 2013.
37. Edgar RC. Search and clustering orders of magnitude faster than BLAST. *Bioinformatics*. 2010;26(19):2460-2461.
38. Wang Q, Garrity GM, Tiedje JM, Cole JR. Naive Bayesian classifier for rapid assignment of rRNA sequences into the new bacterial taxonomy. *Applied and Environmental Microbiology*. 2007;73(16):5261-5267.
39. Prantl L, Schreml S, Fichtner-Feigl S, et al. Clinical and morphological conditions in capsular contracture formed around silicone breast implants. *Plastic and Reconstructive Surgery*. 2007;120(1):275-284.
40. Guijarro-Martinez R, Miragall Alba L, Marques Mateo M, Puche Torres M, Pascual Gil JV. Autologous fat transfer to the cranio-maxillofacial region: updates and controversies. *Journal of cranio-maxillo-facial Surgery: Official Publication of the European Association for Cranio-Maxillo-Facial Surgery*. 2011;39(5):359-363.
41. Myckatyn TM, Cavallo JA, Sharma K, et al. The impact of chemotherapy and radiation therapy on the remodeling of acellular dermal matrices in staged, prosthetic breast reconstruction. *Plastic and Reconstructive Surgery*. 2015;135(1):43e-57e.
42. Valentin JE, Badylak JS, McCabe GP, Badylak SF. Extracellular matrix bioscaffolds for orthopaedic applications. A comparative histologic study. *J Bone Joint Surg Am*. 2006;88(12):2673-2686.
43. Cavallo JA, Greco SC, Liu J, Frisella MM, Deeken CR, Matthews BD. Remodeling characteristics and biomechanical properties of a crosslinked versus a non-crosslinked porcine dermis scaffolds in a porcine model of ventral hernia repair. *Hernia*. 2013. PubMed PMID: 23483265.
44. Cavallo JA, Roma AA, Jasielec MS, et al. Remodeling characteristics and collagen distribution in biologic scaffold materials explanted from human subjects after abdominal soft tissue reconstruction: an analysis of scaffold remodeling characteristics by patient risk factors and surgical site classifications. *Surg Endosc*. 2014;28 (6):1852-1865.
45. Brown SR, Melman L, Jenkins E, et al. Collagen type I:III ratio of the gastroesophageal junction in patients with paraesophageal hernias. *Surgical Endoscopy*. 2011;25 (5):1390-1394.
46. Cho H, Jonsson H, Campbell K, et al. Self-organization in high-density bacterial colonies: efficient crowd control. *PLoS Biol*. 2007;5(11):e302.
47. Bester E, Kroukamp O, Wolfaardt GM, Boonzaaier L, Liss SN. Metabolic differentiation in biofilms as indicated by carbon dioxide production rates. *Applied and Environmental Microbiology*. 2010;76(4):1189-1197.
48. Onyango LA, Hugh Dunstan R, Roberts TK, Macdonald MMGottfries J. Phenotypic variants of staphylococci and their underlying population distributions following exposure to stress. *PloS one*. 2013;8(10):e77614.

49. Bengtson BP, Van Natta BW, Murphy DK, Slicton A, Maxwell GP. Style 410 highly cohesive silicone breast implant core study results at 3 years. *Plastic and Reconstructive Surgery*. 2007;120(7 Suppl 1):40S-48S.
50. Cunningham B, McCue J. Safety and effectiveness of Mentor's MemoryGel implants at 6 years. *Aesthetic Plastic Surgery*. 2009;33(3):440-444.
51. Spear SL, Murphy DK, Allergan Silicone Breast Implant USCCSG. Natrelle round silicone breast implants: core study results at 10 years. *Plastic and Reconstructive Surgery*. 2014;133(6):1354-1361.
52. Niechajev I, Jurell G, Lohjelm L. Prospective study comparing two brands of cohesive gel breast implants with anatomic shape: 5-year follow-up evaluation. *Aesthetic Plastic Surgery*. 2007;31(6):697-710.
53. Stevens WG, Nahabedian MY, Calobrace MB, et al. Risk factor analysis for capsular contracture: a 5-year Sientra study analysis using round, smooth, and textured implants for breast augmentation. *Plastic and Reconstructive Surgery*. 2013;132(5):1115-1123.
54. Prantl L, Englbrecht MA, Schoeneich M, Kuehlmann B, Jung EM, Kubale R. Semiquantitative measurements of capsular contracture with elastography - First results in correlation to Baker Score. *Clin Hemorheol Microcirc*. 2014;58(4):521-528.
55. Katzel EB, Koltz PF, Tierney R, et al. A novel animal model for studying silicone gel-related capsular contracture. *Plastic and Reconstructive Surgery*. 2010;126(5):1483-1491.
56. Wilflingseder P, Hoinkes G, Mikuz G. Tissue reactions from silicone implant in augmentation mammaplasties. *Minerva Chir*. 1983;38(12):877-880.
57. Bergmann PA, Liodaki ME, Mauss KL, et al. [Histological and immunohistochemical study of capsular contracture in an animal model—a comparison of two implants according to a modification of Wilflingseder's classification]. *Handchirurgie, Mikrochirurgie, plastische Chirurgie : Organ der Deutschsprachigen Arbeitsgemeinschaft fur Handchirurgie : Organ der Deutschsprachigen Arbeitsgemeinschaft fur Mikrochirurgie der Peripheren Nerven und Gefasse* 2012;44(4):220-226.
58. Bergmann PA, Tamouridis G, Lohmeyer JA, et al. The effect of a bacterial contamination on the formation of capsular contracture with polyurethane breast implants in comparison with textured silicone implants: an animal study. *Journal of Plastic, Reconstructive and Aesthetic Surgery: JPRAS*. 2014;67(10):1364-1370.
59. Siehnel R, Traxler B, An DD, Parsek MR, Schaefer AL, Singh PK. A unique regulator controls the activation threshold of quorum-regulated genes in Pseudomonas aeruginosa. *Proceedings of the National Academy of Sciences of the United States of America*. 2010;107(17): 7916-7921.
60. Singh PK, Schaefer AL, Parsek MR, Moninger TO, Welsh MJGreenberg EP. Quorum-sensing signals indicate that cystic fibrosis lungs are infected with bacterial biofilms. *Nature*. 2000;407(6805):762-764.
61. Lewis K. Persister cells, dormancy and infectious disease. *Nature Reviews. Microbiology*. 2007;5(1):48-56.
62. Wood TK, Knabel SJ, Kwan BW. Bacterial persister cell formation and dormancy. *Applied and Environmental Microbiology*. 2013;79(23):7116-7121.
63. Kint CI, Verstraeten N, Fauvart M, Michiels J. New-found fundamentals of bacterial persistence. *Trends in Microbiology*. 2012;20(12):577-585.
64. Vega NM, Allison KR, Khalil AS, Collins JJ. Signaling-mediated bacterial persister formation. *Nature Chemical Biology*. 2012;8(5):431-433.
65. Hall-Stoodley L, Costerton JW, Stoodley P. Bacterial biofilms: from the natural environment to infectious diseases. Nature Reviews. Microbiology. 2004;2(2):95-108.
66. Karau MJ, Greenwood-Quaintance KE, Schmidt SM, et al. Microbial biofilms and breast tissue expanders. *BioMed Research International*. 2013;2013:254940.
67. Jhass AK, Johnston DA, Gulati A, Anand R, Stoodley P, Sharma S. A scanning electron microscope characterisation of biofilm on failed craniofacial osteosynthesis miniplates. *J Craniomaxillofac Surg*. 2014;42(7):e372-e378.
68. Kossovsky N, Heggers JP, Parsons RW, Robson MC. Acceleration of capsule formation around silicone implants by infection in a guinea pig model. *Plastic and Reconstructive Surgery*. 1984;73(1):91-98.
69. Burkhardt BR, Fried M, Schnur PL, Tofield JJ. Capsules, infection, and intraluminal antibiotics. *Plastic and Reconstructive Surgery*. 1981;68(1):43-49.
70. Shah Z, Lehman JA Jr., Tan J. Does infection play a role in breast capsular contracture? *Plastic and Reconstructive Surgery*. 1981;68(1):34-42.
71. Hurwitz PJ. Chronic infection as a possible cause of capsular contracture. *Plastic and Reconstructive Surgery*. 1987;79(3):504-505.
72. Virden CP, Dobke MK, Stein P, Parsons CL, Frank DH. Subclinical infection of the silicone breast implant surface as a possible cause of capsular contracture. *Aesthetic Plastic Surgery*. 1992;16(2):173-179.
73. Netscher DT, Weizer G, Wigoda P, Walker LE, Thornby J, Bowen D. Clinical relevance of positive breast periprosthetic cultures without overt infection. *Plastic and Reconstructive Surgery*. 1995;96(5):1125-1129.
74. Aad G, Abbott B, Abdallah J, et al. Search for diphoton events with large missing transverse energy in 7 TeV proton-proton collisions with the ATLAS detector. *Physical Review Letters*. 2011;106(12):121803.
75. Rieger UM, Pierer G, Luscher NJ, Trampuz A. Sonication of removed breast implants for improved detection of subclinical infection. *Aesthetic Plastic Surgery*. 2009;33 (3):404-408.
76. Schreml S, Heine N, Eisenmann-Klein M, Prantl L. Bacterial colonization is of major relevance for high-grade capsular contracture after augmentation mammaplasty. *Annals of Plastic Surgery*. 2007;59(2):126-130.
77. Del Pozo JL, Tran NV, Petty PM, et al. Pilot study of association of bacteria on breast implants with capsular contracture. *J Clin Microbiol*. 2009;47(5):1333-1337.
78. Costerton JW, Stewart PS, Greenberg EP. Bacterial biofilms: a common cause of persistent infections. *Science*. 1999;284(5418):1318-1322.

79. Amann RI, Ludwig W, Schleifer KH. Phylogenetic identification and in situ detection of individual microbial cells without cultivation. *Microbiological Reviews*. 1995;59 (1):143-169.
80. Nistico L, Hall-Stoodley L, Stoodley P. Imaging bacteria and biofilms on hardware and periprosthetic tissue in orthopedic infections. *Methods Mol Biol*. 2014;1147:105-126.
81. Hall-Stoodley L, Stoodley P, Kathju S, et al. Towards diagnostic guidelines for biofilm-associated infections. *FEMS Immunology and Medical Microbiology*. 2012;65(2):127-145.
82. Nistico L, Gieseke A, Stoodley P, Hall-Stoodley L, Kerschner JE, Ehrlich GD. Fluorescence "in situ" hybridization for the detection of biofilm in the middle ear and upper respiratory tract mucosa. *Methods Mol Biol*. 2009;493:191-213.
83. Stoodley P, Conti SF, DeMeo PJ, et al. Characterization of a mixed MRSA/MRSE biofilm in an explanted total ankle arthroplasty. *FEMS Immunology and Medical Microbiology*. 2011;62(1):66-74.
84. Stoodley P, Kathju S, Hu FZ, et al. Molecular and imaging techniques for bacterial biofilms in joint arthroplasty infections. *Clinical Orthopaedics and Related Research*. 2005(437):31-40.
85. Constantine RS, Constantine FC, Rohrich RJ. The ever-changing role of biofilms in plastic surgery. *Plastic and Reconstructive Surgery*. 2014;133(6):865e-872e.
86. Hoa M, Tomovic S, Nistico L, et al. Identification of adenoid biofilms with middle ear pathogens in otitis-prone children utilizing SEM and FISH. *International Journal of Pediatric Otorhinolaryngology*. 2009;73(9):1242-1248.
87. McConoughey SJ, Howlin R, Granger JF, et al. Biofilms in periprosthetic orthopedic infections. *Future Microbiology*. 2014;9:987-1007.
88. Kathju S, Nistico L, Tower I, Lasko LA, Stoodley P. Bacterial biofilms on implanted suture material are a cause of surgical site infection. *Surgical Infections*. 2014;15(5):592-600.
89. Monsen T, Lovgren E, Widerstrom M, Wallinder L. In vitro effect of ultrasound on bacteria and suggested protocol for sonication and diagnosis of prosthetic infections. *J Clin Microbiol*. 2009;47(8):2496-2501.
90. Post JC, Preston RA, Aul JJ, et al. Molecular analysis of bacterial pathogens in otitis media with effusion. *JAMA*. 1995;273(20):1598-1604.
91. Hall-Stoodley L, Hu FZ, Gieseke A, et al. Direct detection of bacterial biofilms on the middle-ear mucosa of children with chronic otitis media. *JAMA*. 2006;296(2):202-211.
92. Trampuz A, Piper KE, Jacobson MJ, et al. Sonication of removed hip and knee prostheses for diagnosis of infection. *The New England journal of medicine*. 2007;357 (7):654-663.
93. Nistco L, Hall-Stoodley L, Stoodley P. *Imaging bacteria and biofilms on hardware and periprosthetic tissue in orthopedic infections*. New York: Humana Press; 2014.
94. Hoffman LR, D'Argenio DA, MacCoss MJ, Zhang Z, Jones RAMiller SI. Aminoglycoside antibiotics induce bacterial biofilm formation. *Nature*. 2005;436(7054):1171-1175.
95. Kaplan JB. Antibiotic-induced biofilm formation. *Int J Artif Organs*. 2011;34(9):737-751.
96. Ghigo JM. Natural conjugative plasmids induce bacterial biofilm development. *Nature*. 2001;412(6845):442-445.
97. Drinane JJ, Bergman RS, Folkers BL, Kortes MJ. Revisiting Triple Antibiotic Irrigation of Breast Implant Pockets: A Placebo-controlled Single Practice Cohort Study. *Plastic and Reconstructive Surgery. Global Open*. 2013;1(7):e55.
98. Drinane JJ, Kortes MJ, Bergman RS, Folkers BL. Evaluation of Antibiotic Irrigation Versus Saline Irrigation in Reducing the Long-Term Incidence and Severity of Capsular Contraction After Primary Augmentation Mammoplasty. *Annals of Plastic Surgery*. 2014. Epub ahead of print. PMID: 25144414.
99. Liao EC, Nyame T, Lemon KP, Kolter R. High Throughput Assay for Bacterial Biofilm Formation on Biomaterials. *Plastic and Reconstructive Surgery*. 2009;124(4S):107.